

Direct measurement of the terrestrial ${}^7\text{Be}$ L/K capture ratio in cryogenic tantalum

S. Fretwell,¹ K.G. Leach,^{1,*} C. Bray,¹ G.B. Kim,² J. Dilling,³ A. Lennarz,³
X. Mougeot,⁴ F. Ponce,^{5,2} C. Ruiz,³ J. Stackhouse,¹ and S. Friedrich²

¹*Department of Physics, Colorado School of Mines, Golden, CO 80401, USA*

²*Nuclear and Chemical Sciences Division, Lawrence Livermore National Laboratory, Livermore, CA 94550, USA*

³*TRIUMF, 4004 Wesbrook Mall, Vancouver, BC V6T 2A3, Canada*

⁴*CEA, LIST, Laboratoire National Henri Becquerel (LNE-LNHB), CEA-Saclay 91191 Gif-sur-Yvette Cedex, France*

⁵*Department of Physics, Stanford University, Stanford, CA 94305, USA*

(Dated: July 5, 2022)

We report a high-statistics measurement of the L/K orbital electron capture (EC) ratio in ${}^7\text{Be}$ embedded in cryogenic Ta. The thin Ta film formed part of a high-resolution superconducting tunnel junction (STJ) radiation detector that was used to identify the signals from different decay channels. The measured L/K capture ratio of 0.070(7) is significantly larger than the only previous measurement of this quantity and the theoretical predictions that include in-medium effects. This result brings into question the accuracy of the extrapolated L/K ratio currently used in calculations of the ${}^7\text{Be}$ destruction rate in astrophysical environments relevant to solar and galactic neutrino modeling, and the cosmological lithium problem. This Letter presents the first experiment that uses STJs for nuclear-recoil detection, opening a new experimental avenue for low-energy precision measurements with rare isotopes.

In the core of low-mass main-sequence stars such as the Sun, the dominant energy-production mechanism is the so-called proton - proton chain reaction, or pp chain [1]. This set of reactions initiates roughly 99% of the total energy generation in the Sun through fusion, and thus has significant importance within the Solar Standard Model (SSM) [2]. In the pp chain, ${}^7\text{Be}$ is produced via ${}^3\text{He}+{}^4\text{He}$ fusion, a process that is experimentally well constrained [1]. The main destruction mechanism of ${}^7\text{Be}$ at solar core temperatures occurs in the second branch of the pp chain (pp -II) via the weak-interaction process of electron-capture (EC): ${}^7\text{Be}+e^- \rightarrow {}^7\text{Li}+\nu_e$. This is the dominant form of Li production in the Sun, and produces discrete lines in the solar neutrino spectrum [3]. Recent work has also confirmed that ${}^7\text{Be}$ production and decay in novae is the dominant form of ${}^7\text{Li}$ generation in our galaxy [4]. This was possible via direct observation of ${}^7\text{Be}$ -II spectral lines, enabling determination of the mass fraction of ejected ${}^7\text{Be}$ in several novae and their comparison to hydrodynamic nova models. Thus, the EC decay of ${}^7\text{Be}$ is of interest to a number of solar neutrino models [5] and the cosmological lithium problem [6, 7]. One important issue for these studies is obtaining reliable estimates for the rate of ${}^7\text{Be}$ EC in the aforementioned astrophysical environments. Existing values differ dramatically from terrestrial laboratory measurements since the atoms are typically highly ionized and the environmental electron densities are high [1, 6]. The theoretical evaluations must therefore account not only for the nuclear interaction, but also the processes in which ${}^7\text{Be}$ ions and electrons interact, and thus require benchmarking to terrestrial conditions where data exist. In particular, the spatial extent of the $2s$ electronic orbit plays a major role in such estimates [8], and thus direct measurements of the L/K capture ratio can provide important experi-

mental constraints on the atomic properties of the $1s$ and $2s$ wavefunction overlap with the nuclear volume.

${}^7\text{Be}$ decays by EC primarily to the nuclear ground-state of ${}^7\text{Li}$ with a Q_{EC} -value of 861.89(7) keV [9] and a laboratory half-life of $T_{1/2} = 53.22(6)$ days. A small branch of 10.44(4)% results in the population of a short-lived excited nuclear state in ${}^7\text{Li}$ ($T_{1/2} = 72.8(20)$ fs) [10] that de-excites via emission of a 477.603(2) keV γ -ray [11]. In the EC process, the electron can be captured either from the $1s$ shell (K -capture) or the $2s$ shell of Be (L -capture). For K -capture, the binding energy of the $1s$ hole is subsequently liberated by emission of an Auger electron whose energy adds to the decay signal and separates it from the L -capture signal. Since the nuclear decay and subsequent atomic relaxation occur on short time scales, a direct measurement produces a spectrum with four peaks: two for K -capture and two for L -capture into the ground state and the excited state of ${}^7\text{Li}$, respectively.

The current literature value for the L/K capture ratio in ${}^7\text{Be}$ of 0.040(6) is based on a single direct measurement at 0.06 K using a high-resolution Si microcalorimeter whose HgTe absorber had been implanted with ${}^7\text{Be}$ [12]. At the time of its publication, the measured value was more than a factor of two smaller than the best theoretical estimates. The authors suggested that this deviation from theoretical predictions resulted from a modification of the electron wavefunction due to in-medium effects, where the Be $2s$ wavefunction was altered by implantation into the HgTe matrix. This effect was investigated theoretically in detail for a number of host media and was found to decrease the L/K ratio by up to 80% relative to the value expected in atomic Be [13], even if the total decay half-life remained constant to within better than 1%. This reduction has been found to alter the SSM esti-

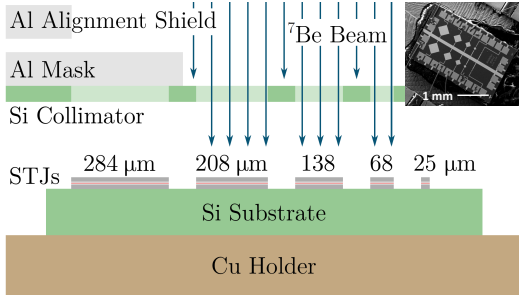


FIG. 1. (Color online) Schematic of the STJ detector chip, Si collimator, and Al mask during ^7Be implantation. The inset shows a scanning electron microscope (SEM) image of the chip used in this experiment.

mates for the ^7Be and ^8B neutrino fluxes by 2.0–2.7% [8]. Given the importance of these L/K capture ratios for the extrapolation of ^7Be EC rates in astrophysical environments, further experimental investigations of these in-medium effects are required. This Letter reports a high-statistics direct measurement of the L/K capture ratio in ^7Be implanted in cryogenic Ta where such in-medium effects are predicted to be large.

Ta-based superconducting tunnel junction (STJ) radiation detectors were used to measure the L/K capture ratio of ^7Be in Ta. The STJs are five-layer devices consisting of Ta (165 nm) - Al (50 nm) - Al_2O_3 (1 nm) - Al (50 nm) - Ta (265 nm) that were fabricated by photolithography at STAR Cryoelectronics LLC [14] (Fig. 1 inset). STJs exploit the small energy gap $\Delta_{\text{Ta}} = 0.7$ meV in superconducting Ta to provide $\sim 30\times$ higher energy resolution than conventional Si or Ge detectors, and can resolve the K -capture from the L -capture signals in the decay.

$^7\text{Be}^+$ ions were implanted into the STJs through Si collimators at TRIUMF's Isotope Separator and Accelerator (ISAC) facility in Vancouver, Canada [15] (Fig. 1). In total, 2×10^8 radioactive $^7\text{Be}^+$ ions were implanted into the $(138 \mu\text{m})^2$ STJ used for the measurements reported here. The ^7Be was produced using the isotope separation on-line (ISOL) technique [16] via spallation reactions from a 10 μA , 480-MeV proton beam incident on a stack of thick uranium carbide targets. The reaction products were released from the target, selectively laser ionized [17], mass-selected, and implanted into the STJs at an energy of 25 keV. This value was limited by bias-voltage instability of the ISAC target module during the scheduled implantation period and resulted in the ions being implanted closer to the surface than initially desired. Stopping Range of Ions in Matter (SRIM) simulations [18] indicate that the mean implantation depth into the Ta layer of each STJ was 46 nm with a straggle of 26 nm.

The decay of ^7Be was measured at a temperature of ~ 0.1 K in an adiabatic demagnetization refrigerator

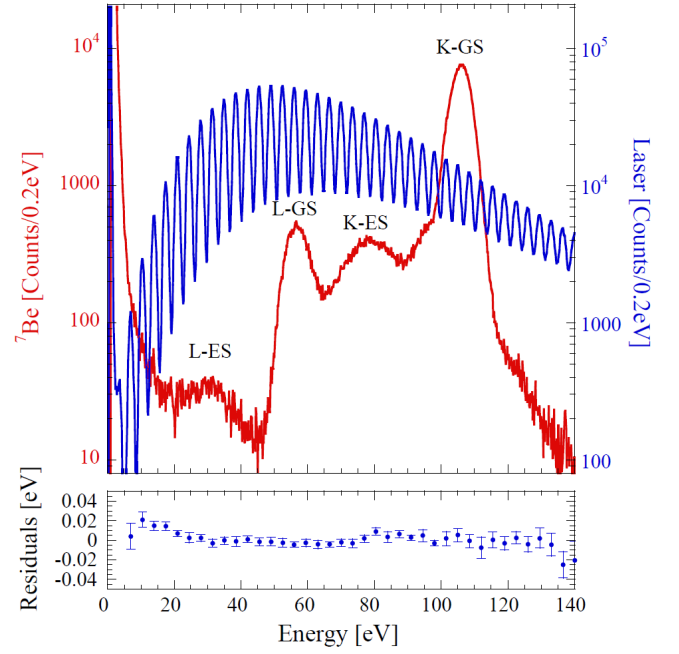


FIG. 2. (Color online) The ^7Li recoil energy spectrum (red) for a single 22 hour run composed of 44 individually calibrated 30-minute spectra. The calibration signal (blue), whose peaks correspond to integer numbers of laser photons per pulse, was measured in coincidence with the laser trigger and the signal from the ^7Be decay in anti-coincidence. The residuals in the bottom panel show a calibration accuracy in the region of interest of better than ± 10 meV.

(ADR) with liquid N_2 and He pre-cooling at Lawrence Livermore National Laboratory (LLNL). For energy calibration, the STJs were simultaneously exposed to 3.49965(15) eV photons from a pulsed Nd:YVO $_4$ laser triggered at a rate of 100 Hz [19]. At this rate, 1% of the total acquisition time was used for calibration. The laser intensity was adjusted such that multi-photon absorption provides a comb of peaks over the energy range of interest from 20 - 120 eV in the $(138 \mu\text{m})^2$ STJ. The signals were read out with a custom-designed current sensitive preamplifier [20], filtered with a spectroscopy amplifier (Ortec 627) with a shaping time of 10 μs and captured with a two-channel nuclear multi-channel analyzer (MCA) (Ortec Aspec927). The laser calibration spectrum was recorded in coincidence with the laser trigger and the ^7Be decay signal in anti-coincidence (Fig. 2).

Data were acquired for ~ 20 hours/day over a period of one month. ^7Be recoil spectra and their corresponding laser calibration were recorded every 30 minutes so that they could be calibrated individually to correct for small drifts in the detector response. For this, the laser signal was fit to a superposition of Gaussian functions, each corresponding to an integer multiple of the single photon energy. The measured Gaussian centroids scale linearly

with energy, with a small non-linearity of order 10^{-4} per eV [21]. Laser peaks below 20 eV and above 120 eV were omitted from the calibration because they have poor statistics in the individual 30-minute spectra. The calibrated spectra were re-binned to 0.2 eV and summed. The ^7Be spectrum and its laser calibration from a single day of data are shown in Fig. 2. The laser peaks are well separated, with the energy resolution increasing from 1.4 eV to 2.9 eV full-width at half-maximum (FWHM) in the energy range up to 140 eV. For energies between 20 and 120 eV, the residuals to the calibration have an average uncertainty ≤ 10 meV that sets the calibration accuracy of the spectrum.

To first order, the ^7Li recoil spectrum is well described by the four peaks generated by the two nuclear and two atomic processes: K -capture to the nuclear ground-state (K-GS), K -capture to the nuclear excited-state (K-ES), L -capture to the nuclear ground-state (L-GS), and L -capture to the nuclear excited state (L-ES). Both decays to the excited nuclear state in ^7Li display Doppler-broadened recoil peaks due to the isotropic γ -decay in-flight prior to stopping. In addition to these four peaks, the sudden change in Z following EC decay also results in the electrons not being in an eigenstate of the daughter atom [22]. This can cause the remaining electron(s) to undergo *shake-up* into a bound state of Li or *shake-off* into the continuum [23] and generate a high-energy tail above each peak [24].

The K-GS and L-GS peaks were found to be roughly four times wider than the resolution of the laser peaks. Detector drift may account for at most ~ 0.5 eV of this difference. Other sources of broadening are from variations in the Li $1s$ and $2s$ binding energies for Li atoms at different sites in the Ta lattice, or by varying self-recombination of the excess quasiparticles in the region of reduced gap due to localized energy deposition of the recoil [25]. Further, the energy difference between the L-GS and the K-GS peaks was measured to be 49.27(6) eV, significantly lower than the binding energy of the Li $1s$ level of 54.74(2) eV [26]. This is either due to in-medium effects of the Li in Ta or an inconsistency in the literature value [26, 27]. Both the origin of the line broadening and the binding energy discrepancy will be investigated in future work.

In addition, a broad background is visible at low energies that decreases as a function of energy. This background is due to 478 keV γ -rays from the decay of the ^7Li excited state that interact in the Si substrate below the STJ detector (Fig. 1). High-energy phonons generated in these interactions can propagate to the STJ detectors before thermalization and break Cooper pairs in the detector electrodes. The resulting signals are determined by the deposited energy and the distance between the interaction location and the STJ. A low-energy tail is also visible below the K-GS peak. This tail has different shapes depending on which STJ detector is used, indi-

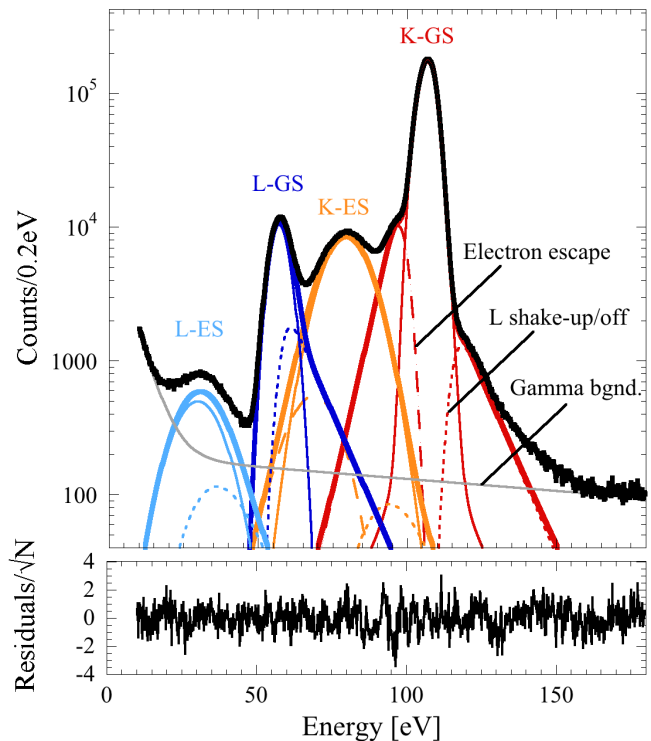


FIG. 3. (Color online) The summed ^7Li recoil spectrum of all individually calibrated 1-day spectra from a single $(138 \mu\text{m})^2$ STJ detector. In addition to the four primary peaks (solid lines), the K -capture peaks have low-energy tails due to electron escape (dashed lines), and all peaks have a high-energy tail from electron shake-up and shake-off effects (dotted lines). The fit residuals in the bottom panel are normalized by the statistical error of the measurement ($\chi^2/\nu = 0.95$).

cating that it is not intrinsic to the ^7Be decay but due to some form of energy loss through the detector surface which varies for each STJ. Since no tail is observed below the L-GS peak, the low-energy tail below the K-GS peak is likely caused by partial escape of the energy of the Auger electron that is produced in the relaxation of the $1s$ core hole. This results from the relatively low implantation depth of the ^7Be atoms causing a significant fraction of the decays to occur within ~ 10 nm of the detector surface. A similar low-energy tail is expected to also accompany the K-ES peak. These additional features increase the difficulty in extracting the L/K ratio from the experimental data since the exact shapes of the γ -ray background and escape tails are not known.

The resulting recoil-energy spectrum from all runs, energy calibrated and summed, is shown in Fig. 3. For the two ground-state decay peaks, three Gaussian functions were used to fit the edges of the distributions, which may reflect the broadening of the peaks due to in-medium effects. The two excited-state peaks are well described by the same set of Gaussian distributions but with a Doppler-broadened width. All K -capture Gaussian func-

tions were convolved with the Lorentzian lineshape of the Auger process defined by the lifetime of the Li 1s core hole [28]. To aid in the fit convergence, the known branching fraction of EC decay to the nuclear excited-state in ${}^7\text{Li}$ [10] was used to constrain the area ratios of the excited-state to ground-state for both K - and L -capture. The L -electron shake-up and shake-off tails for all four peaks were approximated by an exponential decay convolved with the width of the corresponding peak. The tail areas and decay constants were constrained to the same value respectively for the two K - and the two L -capture peaks. Similarly, the electron escape following Auger emission was modeled by exponentially-decaying tails below the K -capture peaks, again broadened by the widths of the K -GS and K -ES peak, respectively. Finally, the γ -ray background was described by a sum of two exponential functions based on spectra from the STJ detectors without ${}^7\text{Be}$, as well as previous work with the same detectors [19].

The fit was performed on the data from 10 to 180 eV with a least-squares regression within the Python IMINUIT framework [29, 30]. The best fit is presented with the data in Fig. 3, and resulted in $L/K = 0.07165(29)_{\text{stat.}}$ with $\chi^2/\nu = 0.95$. In order to investigate the systematic uncertainties in the L/K ratio that result from the choice in peak shape and exponential tails, the functions and constraints of the fit were systematically varied over a range of plausible alternatives. This included using two instead of three Gaussian functions for the central peaks (both with and without steep exponential tails). More importantly, different constraints on the areas of the shake-up/shake-off tails were included, because when left unconstrained, all fits converged to a larger tail above the L -capture peaks than above the K -capture peaks (Fig. 3).

For K -capture, the shaking areas were found to be between 1.1% and 2.8% while the L -capture shaking minimized to a much larger range from 1.2% to 31.5%. It is this difference that ultimately dominates the systematic uncertainty in the L/K ratio. These variations could simply reflect that the variation in the Li 2s energy levels in the Ta matrix is larger than the spread of the Li 1s levels, although a distribution of well above 10 eV does seem unrealistically wide. Alternatively, the L shake-up and shake-off effects could be stronger for L -capture than for K -capture events, although this is in disagreement with theoretical estimates and thus also unlikely. Finally, the 60-70 eV region could be affected by an electron escape tail that does not decay exponentially to zero but has an increased probability for high energies. This could reflect that a small fraction of Auger electrons escape from the detector with almost all of their energy since $\leq 1\%$ of the ${}^7\text{Be}$ atoms were implanted within the mean free path of ~ 1 nm of the surface [31]. The different fits resulted in a spread of the L/K ratio of 0.064 to 0.078 with reduced χ^2 values of between 0.95 and 1.41. This range

is dominated by the uncertainty of the fit in region from 60 to 70 eV and reflects L/K ratios that are consistent with the data for a variety of assumptions in the underlying physics. Taking into account these differences, we determine a value of $L/K = 0.0702(66)_{\text{sys.}}(3)_{\text{stat.}}$.

The measured value of $L/K = 0.070(7)$ reported here is nearly a factor of 2 larger than the only previous measurement of 0.040(4) in HgTe [12]. We performed a precise new calculation of the L/K ratio for ${}^7\text{Be}$ decay “in-vacuum” using the method detailed in Refs. [32, 33], which yields a value of $L/K = 0.105(8)$. For ${}^7\text{Be}$ in Ta, in-medium effects are expected to change this value by a factor of 0.2986 [13] to $L/K = 0.031(2)$. This is more than 2 times (4σ) smaller than the measured value presented here. The discrepancy between the theoretical estimates for the capture ratio in ${}^7\text{Be}$ and the experimental results likely points to a deficiency in the models that are used to correct for in-medium effects. Since the measured L/K ratio is an important empirical input for understanding the rate at which ${}^7\text{Li}$ is created in the Universe, the implications of such estimates being incorrect may be significant. Finally, these measurements demonstrate that high-resolution STJ detectors show tremendous promise for nuclear recoil experiments in precision low-energy subatomic physics.

This work was funded by the LLNL LDRD program through grants 19-FS-027 and 20-LW-006 and the U.S. Department of Energy Office of Science under contract DE-SC0017649. TRIUMF receives federal funding via a contribution agreement with the National Research Council of Canada (NRC). This work was performed under the auspices of the U.S. Department of Energy by Lawrence Livermore National Laboratory under Contract DE-AC52-07NA27344. The theoretical work was performed as part of the EMPIR project 17FUN02 MetroMMC. This project has received funding from the EMPIR programme co-financed by the participating states and from the European Union’s Horizon 2020 research and innovation programme. We would like to thank Friedhelm Ames, Louis Clark, Peter Kunz, Jens Lassen, and Brad Schultz for their efforts in facilitating the ion-beam implantation. KGL also thanks Tibor Kibedi, Uwe Greife, John Behr, Fred Sarazin, Vladan Stefanovic, Mark Lusk, Xerxes Stirer, and Jeremy Zimmerman for useful discussions.

* kleach@mines.edu

- [1] E. G. Adelberger, A. García, R. G. H. Robertson, K. A. Snover, A. B. Balantekin, K. Heeger, M. J. Ramsey-Musolf, D. Bemmerer, A. Junghans, C. A. Bertulani, J.-W. Chen, H. Costantini, P. Prati, M. Couder, E. Uberseder, M. Wiescher, R. Cyburt, B. Davids, S. J. Freedman, M. Gai, D. Gazit, L. Gialanella, G. Imbriani, U. Greife, M. Hass, W. C. Haxton, T. Itahashi,

- K. Kubodera, K. Langanke, D. Leitner, M. Leitner, P. Vetter, L. Winslow, L. E. Marcucci, T. Motobayashi, A. Mukhamedzhanov, R. E. Tribble, K. M. Nollett, F. M. Nunes, T.-S. Park, P. D. Parker, R. Schiavilla, E. C. Simpson, C. Spitaleri, F. Strieder, H.-P. Trautvetter, K. Suemmerer, and S. Typel, *Rev. Mod. Phys.* **83**, 195 (2011).
- [2] J. N. Bahcall, M. H. Pinsonneault, and S. Basu, *The Astrophysical Journal* **555**, 990 (2001).
- [3] M. Agostini, K. Altenmüller, S. Appel, V. Atroshchenko, Z. Bagdasarian, D. Basilico, G. Bellini, J. Benziger, D. Bick, G. Bonfini, D. Bravo, B. Caccianiga, F. Calaprice, A. Caminata, S. Caprioli, M. Carlini, P. Cavalcante, A. Chepurinov, K. Choi, L. Collica, D. D'Angelo, S. Davini, A. Derbin, X. F. Ding, A. Di Ludovico, L. Di Noto, I. Drachnev, K. Fomenko, A. Formozov, D. Franco, F. Gabriele, C. Galbiati, C. Ghiano, M. Giammarchi, A. Goretti, M. Gromov, D. Guffanti, C. Hagner, T. Houdy, E. Hungerford, A. Ianni, A. Ianni, A. Jany, D. Jeschke, V. Kobychiev, D. Korabiev, G. Korga, D. Kryn, M. Laubenstein, E. Litvinovich, F. Lombardi, P. Lombardi, L. Ludhova, G. Lukyanchenko, L. Lukyanchenko, I. Machulin, G. Manuzio, S. Marcocci, J. Martyn, E. Meroni, M. Meyer, L. Miramonti, M. Misiaszek, V. Muratova, B. Neumair, L. Oberauer, B. Opitz, V. Orekhov, F. Ortica, M. Pallavicini, L. Papp, Ö. Penek, N. Pilipenko, A. Pocar, A. Porcelli, G. Raikov, G. Ranucci, A. Razeto, A. Re, M. Redchuk, A. Romani, R. Roncin, N. Rossi, S. Schönert, D. Semenov, M. Skorokhvatov, O. Smirnov, A. Sotnikov, L. F. F. Stokes, Y. Suvorov, R. Tartaglia, G. Testera, J. Thurn, M. Toropova, E. Unzhakov, F. L. Villante, A. Vishneva, R. B. Vogelaar, F. von Feilitzsch, H. Wang, S. Weinz, M. Wojcik, M. Wurm, Z. Yokley, O. Zaimidoroga, S. Zavatarelli, K. Zuber, G. Zuzel, and T. B. Collaboration, *Nature* **562**, 505 (2018).
- [4] P. Molaro, L. Izzo, P. Bonifacio, M. Hernanz, P. Selvelli, and M. dellaValle, *Monthly Notices of the Royal Astronomical Society* **492**, 4975 (2020), <https://academic.oup.com/mnras/article-pdf/492/4/4975/32355054/stz3587.pdf>.
- [5] D. Vescovi, L. Piersanti, S. Cristallo, M. Busso, F. Vissani, S. Palmerini, S. Simonucci, and S. Taioli, *Astronomy and Astrophysics* **623**, A126 (2019), arXiv:1902.01826 [astro-ph.SR].
- [6] S. Simonucci, S. Taioli, S. Palmerini, and M. Busso, *The Astrophysical Journal* **764**, 118 (2013).
- [7] S. Q. Hou, J. J. He, A. Parikh, D. Kahl, C. A. Bertulani, T. Kajino, G. J. Mathews, and G. Zhao, *The Astrophysical Journal* **834**, 165 (2017).
- [8] P. Das and A. Ray, *Phys. Rev. C* **71**, 025801 (2005).
- [9] M. Wang, G. Audi, F. Kondev, W. Huang, S. Naimi, and X. Xu, *Chinese Physics C* **41**, 030003 (2017).
- [10] D. Tilley, C. Cheves, J. Godwin, G. Hale, H. Hofmann, J. Kelley, C. Sheu, and H. Weller, *Nuclear Physics A* **708**, 3 (2002).
- [11] R. Helmer and C. van der Leun, *Nuclear Instruments and Methods in Physics Research Section A: Accelerators, Spectrometers, Detectors and Associated Equipment* **450**, 35 (2000).
- [12] P. A. Voytas, C. Ternovan, M. Galeazzi, D. McCammon, J. J. Kolata, P. Santi, D. Peterson, V. Guimarães, F. D. Becchetti, M. Y. Lee, T. W. O'Donnell, D. A. Roberts, and S. Shaheen, *Phys. Rev. Lett.* **88**, 012501 (2001).
- [13] A. Ray, P. Das, S. K. Saha, S. K. Das, and A. Mookerjee, *Phys. Rev. C* **66**, 012501 (2002).
- [14] M. H. Carpenter, S. Friedrich, J. A. Hall, J. Harris, W. K. Warburton, and R. Cantor, *IEEE Transactions on Applied Superconductivity* **23**, 2400504 (2013).
- [15] J. Dilling and R. Krücken, *Hyperfine Interactions* **225**, 111 (2014).
- [16] Y. Blumenfeld, T. Nilsson, and P. V. Duppen, *Physica Scripta* **2013**, 014023 (2013).
- [17] J. Lassen, P. Bricault, M. Domsby, J. P. Lavoie, M. Gillner, T. Gottwald, F. Hellbusch, A. Teigelhfer, A. Voss, and K. D. A. Wendt, *AIP Conference Proceedings* **1104**, 9 (2009), <https://aip.scitation.org/doi/pdf/10.1063/1.3115616>.
- [18] J. F. Ziegler, M. Ziegler, and J. Biersack, *Nuclear Instruments and Methods in Physics Research Section B: Beam Interactions with Materials and Atoms* **268**, 1818 (2010), 19th International Conference on Ion Beam Analysis.
- [19] F. Ponce, E. Swanberg, J. Burke, R. Henderson, and S. Friedrich, *Phys. Rev. C* **97**, 054310 (2018).
- [20] W. Warburton, J. Harris, and S. Friedrich, *Nuclear Instruments and Methods in Physics Research Section A: Accelerators, Spectrometers, Detectors and Associated Equipment* **784**, 236 (2015), symposium on Radiation Measurements and Applications 2014 (SORMA XV).
- [21] S. Friedrich, F. Ponce, J. A. Hall, and R. Cantor, *Journal of Low Temperature Physics* (2020), 10.1007/s10909-020-02360-2.
- [22] T. A. Carlson, C. W. Nestor, T. C. Tucker, and F. B. Malik, *Phys. Rev.* **169**, 27 (1968).
- [23] W. Bambynek, H. Behrens, M. H. Chen, B. Crasemann, M. L. Fitzpatrick, K. W. D. Ledingham, H. Genz, M. Mutterer, and R. L. Intemann, *Rev. Mod. Phys.* **49**, 77 (1977).
- [24] J. Law and J. Campbell, *Nuclear Physics A* **199**, 481 (1973).
- [25] A. Zehnder, *Phys. Rev. B* **52**, 12858 (1995).
- [26] J. A. Bearden and A. F. Burr, *Rev. Mod. Phys.* **39**, 125 (1967).
- [27] M. Siegbahn and T. Magnusson, *Zeitschrift für Physik* **87**, 291 (1934).
- [28] P. H. Citrin, G. K. Wertheim, and Y. Baer, *Phys. Rev. B* **16**, 4256 (1977).
- [29] iminuit team, “iminuit – a python interface to minuit,” <https://github.com/scikit-hep/iminuit>, accessed: 2018-03-05.
- [30] F. James and M. Roos, *Computer Physics Communications* **10**, 343 (1975).
- [31] B. Ziaja, R. A. London, and J. Hajdu, *Journal of Applied Physics* **99**, 033514 (2006), <https://doi.org/10.1063/1.2161821>.
- [32] X. Mougeot, *Applied Radiation and Isotopes* **134**, 225 (2018), iCRM 2017 Proceedings of the 21st International Conference on Radionuclide Metrology and its Applications.
- [33] X. Mougeot, *Applied Radiation and Isotopes* **154**, 108884 (2019).